Temperature and Force Dependence of Nanoscale Electron Transport *via* the Cu Protein Azurin

Wenjie Li,[†] Lior Sepunaru,[†,‡] Nadav Amdursky,[†,‡] Sidney R. Cohen,[⊥] Israel Pecht,[§] Mordechai Sheves,[‡,*] and David Cahen[†,*]

[†]Department of Materials & Interfaces, [‡]Department of Organic Chemistry, [⊥]Chemical Research Support, and [§]Department of Immunology, Weizmann Institute of Science, Rehovot 76100, Israel

ABSTRACT Solid-state electron transport (ETp) *via* a monolayer of immobilized azurin (Az) was examined by conducting probe atomic force microscopy (CP-AFM), as a function of both temperature (248−373K) and applied tip force (6−15 nN). At low forces, ETp *via* holo-Az (with Cu^{2+}) is temperature-independent, but thermally activated *via* the Cu-depleted form of Az, apo-Az. While this observation agrees with those of macroscopic-scale measurements, we find that for holo-Az the mechanism of ETp at high temperatures changes upon an increase in the force applied by the tip to the proteins; namely, above 310 K and forces >6 nN ETp becomes thermally activated. This is in contrast to apo-Az, where increasing applied force causes only small monotonic increases in currents due to decreased electrode separation. The distinct ETp temperature dependence of holo- and apo-Az is assigned to a difference in structural response to pressure between the two protein forms. An important implication of these CP-AFM results (of measurements over a *significant* temperature range) is that for reliable ETp measurements on flexible macromolecules, such as proteins, the pressure applied during the measurements should be controlled or at least monitored.

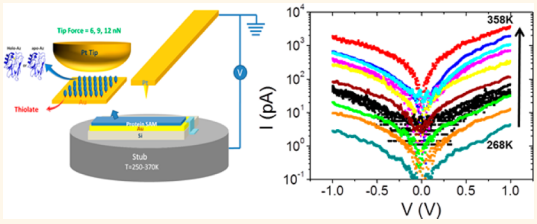

KEYWORDS: nanometer scale · conductivity · azurin · biomolecular electronics · Arrhenius activation energy · tunneling · electron transport

Azurin (Az) is an electron-mediating protein, functional in the bacterial energy conversion system, which has been studied extensively, mostly by spectroscopic[1−3] and electrochemical measurements[4−10] in solution, as a model system for electron transfer (ET) *via* proteins. Solid-state electron transport (ETp) measurements have been reported on several types of proteins,[11−13] including Az, which has been investigated quite intensively, both by nanoscale techniques[14−19] and by macro-scale electrodes.[20−23] Within the latter context we reported recently macroscopic scale ETp measurements *via* Az monolayers,[21] which showed temperature-independent currents *via* holo-Az. ETp *via* the Cu-depleted form of Az, apo-Az, was found to be thermally activated at $T > 180$ K and temperature-independent at $T < 180$ K.

Investigating these current−voltage measurements with nanoscale contacts, may scrutinize two important issues: (i) While the observed temperature independence of the currents through a 3.5 nm thick protein (see later) was quite remarkable, we sought a different measurement method, less likely to be influenced by possible defects (in the monolayer), to ensure that this is indeed an intrinsic property of Az. (ii) Use of conducting probe atomic force microscopy, CP-AFM, allows acquisition of information on the ETp under different pressures applied to the protein. Up to now, only a simple (distance-related) connection between tunneling currents and the force applied to an organic monolayer was found.[24,25] Increasing the applied force on proteins (and likely also on other soft materials) may cause structural changes, which should be considered, in addition to the expected decrease in electrode separation that increases current flow.[26] By combining temperature-dependent current transport measurements and the unique AFM capability of force control on a nanoscale contact area, we can use ETp as an indicator for force-dependent structural

* Address correspondence to david.cahen@weizmann.ac.il, Mudi.Sheves@weizmann.ac.il.

Received for review September 10, 2012 and accepted November 8, 2012.

Published online November 08, 2012
10.1021/nn3041705

changes in proteins. These force-dependent measurements can also provide comparison with macroscopic measurements, where only a negligible gravity force and a constant adhesive force (both from the contact pad) act on the proteins. While, in principle, force control in macroscopic measurement on a monolayer is possible, its use is hampered by the fact that even a slight variation in monolayer uniformity may cause penetration of the protein monolayer by the electrode.

In a series of experiments, Davis and co-workers observed ETp through Az by CP-AFM.[14,16−19] From fits of measured $I-V$ curves to Simmons' nonresonant tunneling model they extracted values for barrier height and length of the Az monolayer at different applied tip forces (at room temperature). Along with ETp experiments *via* Az, current−voltage CP-AFM measurements of other protein monolayers in a solid state environment have been reported, and the data were fitted to different ETp models (for example Fowler−Nordheim tunneling[27]).[15,26,28−30] CP-AFM allows measuring ETp through a limited number of molecules, located between the tip and the surface, or attached to the tip, to the surface, or to both. The effective radius of the AFM tip limits the contact area of the measurement, and in the present work we estimate that we measure up to ∼50 Az molecules. Smaller contact area increases the probability of resolving small defect-free areas for measurement. At the same time we sacrifice sensitivity (lower currents), compared to use of the much more sensitive macroscopic electrode measurements that average over a large area. The two approaches can, thus, be viewed as complementary ones.

According to the Marcus theory,[31] k_{ET}, the ET rate constant between a donor (D) and an acceptor (A), is given by

$$k_{ET} \propto H^2_{D-A}(l_{D-A}) \exp(-E_a/k_B T) \qquad (1)$$

where E_a is the activation energy of the process, T is the absolute temperature, k_B is Boltzmann's constant, and $H_{D\text{-}A}$ is the degree of electronic coupling between D and A, which also depends on $l_{D\text{-}A}$ the separation distance between them. While in ET studies $l_{D\text{-}A}$ is the varied parameter, and varying the temperature may be problematic over a wide range (also in view of solvent presence), for ETp the opposite situation holds. The Az is sandwiched between two electrodes and, in our setup, is coordinatively attached to the bottom electrode by a disulfide bridge through its cysteine residue (Cys3 or Cys26). This configuration introduces a defined and fixed distance between the two electrodes, $l = 3.5$ nm, although in CP-AFM measurements one can change the tip−surface distance by applying different probe forces.[32] Using molecular dynamics simulations, Davis and co-workers proposed that the secondary structure of the protein changes drastically upon applying increasing forces to the protein layer.[19]

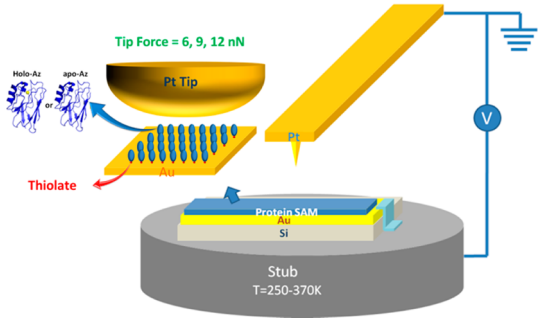

Figure 1. Schematic (not to scale) of junction configuration employed in the ETp measurement *via* the proteins. (PDB ID: 1AZU).

Accordingly, as will be shown and discussed below, at different probe forces, we can expect the medium that separates the tip and the substrate to be affected. This poses a problem for certain nanoscopic measurements, such as those done by dynamic scanning tunneling microscopy (STM),[33] because the protein will be mechanically stressed and possibly structurally affected during most of the measurement. Here we report temperature- and force-dependent CP-AFM of holo- and apo-Az, as a monolayer, in a solid state-like junction over the temperature range of 248−373 K and applied forces of 6−15 nN.

RESULTS

In the employed configuration, a smooth (r.m.s. roughness of ∼0.7 nm over 4 × 4 μm scan) and continuous Au layer is deposited on an H-terminated Si substrate. A self-assembled monolayer of holo- or apo-Az was coupled covalently to the Au substrate *via* S−Au bonding between the Au surface and the relatively exposed cysteine thiolate of Az (Figure 1). To confirm the establishment of the protein monolayer, topographic (amplitude) and phase images were measured in semicontact mode with different amplitude reduction or amplitude set point ratio (97%, 94% and 91%, respectively) (Figure 2). A lower set point ratio corresponds to a higher tip force on the surface. The relative influence of attractive (adhesive) forces changes as the set point ratio is lowered, particularly on compliant surfaces, leading to modification of topography and phase images.[34−36] As we lowered the set point ratio, i.e., increased the tip force, we clearly observed a change in the topography images, and corresponding changes in the phase images. The observed changes in the topography and phase images with different tip forces suggest the presence of a soft layer, that is, proteins. To assess the thickness of the protein monolayer, a square area was scanned in the contact mode with a large feedback force (160 nN). The applied force is sufficiently large to scratch away the monolayer. Following the contact mode scratching procedure we reverted to the semicontact mode to rescan over a larger area, centered around the resulting

trough (Supporting Information, Figure S1a). The obtained image demonstrates that the probe removed the protein over a square area. The cross-section (Supporting Information, Figure S1b) shows that the thickness of the protein layer is about 3.5 nm, the length of Az established by its three-dimensional structure determination.

The measured *I*−*V* of holo- and apo-Az as a function of applied force (conducted at room temperature) is shown in Figure 3. The currents obtained for both proteins increased with probe force. For the holo-Az junctions at 0.5 V bias, the currents ranged between 0.1 and 1 nA for tip forces of 6−15 nN, in agreement with the values reported by Zhao and Davis.[14,19] Clear shorts were observed everywhere with >40 nN tip force, suggesting the tip pinches through the protein layer at this force. The currents across apo-Az junctions spanned a range of 0.002−2 nA for the same force variation. The higher sensitivity of apo-Az to the applied tip force suggests that it is more flexible than holo-Az. Indeed, the structure of apo-Az, though very similar to that of holo-Az, exhibits higher degrees of freedom,[37−40] particularly at the ligand loop near the empty metal binding site (NMR studies).[40] If a low force is applied at room temperature, the observed current across apo-Az junctions at 1 V was an order of magnitude lower than that across the holo-Az junctions (Figure 3, black curve). This difference resembles that obtained in our macroscopic measurements[21] and is qualitatively consistent with results of conduction measurements *via* another metal-containing protein (Ferritin) by CP-AFM,[28] STM,[41] or for Az in a two-terminal configuration.[42] This decrease in current magnitude highlights the role of the Cu ion as an efficient ET and ETp mediator in Az.

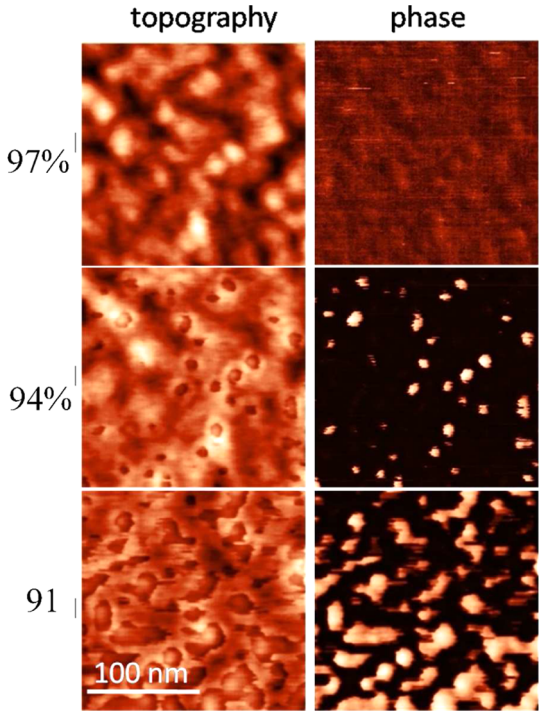

Figure 2. AFM topography (left) and phase (right) images of holo-Az with different amplitude set point ratios (97%, 94%, and 91%, respectively), corresponding to different forces applied on the proteins.

Figure 4 shows the current−voltage characteristics of holo-Az (Figure 4a,b) and the natural logarithm of the currents for voltage sweeps from −1 V to +1 V for apo-Az junctions (Figure 4c,d) as a function of temperature. The *I*−*V* curves were measured over more than 30 random spots for each temperature at constant probe force (6 nN). For each temperature we took the average of all *I*−*V* curves, excluding those exhibiting shorting or insulating behavior (~20%) The distribution of current intensities was normal (inset of Figure 4a); average currents were used for further analysis. The *I*−*V* measurements were performed at each temperature only after the system had remained stable for at least 30 min. As can be seen in Figure 4, holo-Az and apo-Az exhibit distinct ETp characteristics as a function of temperature. The *I*−*V* curves of the holo-Az junctions remained essentially invariant with temperature from 248 to ~370 K (Figure 4a). The measured current *via* the junctions at +0.5 V and −0.5 V as a function of the inverse temperature (Figure 4b) clearly demonstrates a temperature-independent ETp process across holo-Az. Thus, the CP-AFM results, obtained with a relatively low tip force of 6 nN, confirm our macroscopic ETp observations.[21]

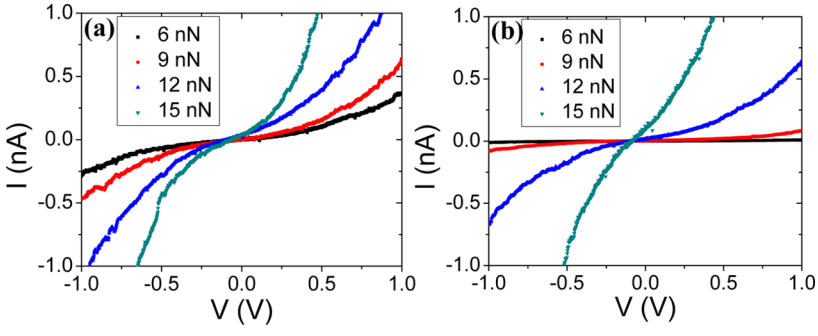

Figure 3. Representative force-dependent *I*−*V* curves of (a) holo-Az and (b) apo-Az at room temperature. The current increases with force from 6 to 15 nN at 1 V are 9.7 ± 2 times and 5.5 × 10^2 ± 3 × 10^2 times for holo-Az and apo-Az, respectively (see Supporting Information for a raw data set).

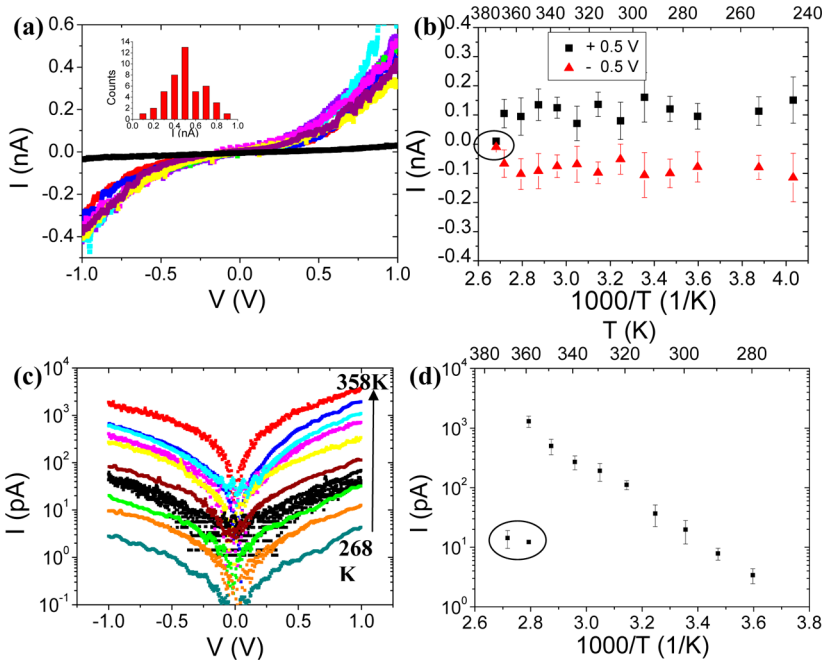

Figure 4. (a) Averaged *I*−*V* curves of holo-Az at temperatures from 248 to 373 K. The inset shows a normal distribution of the currents taken at +1 V. (b) Currents of holo-Az at +0.5 V (black squares) and −0.5 V (red triangles) as a function of inverse temperature. (c) Semilogarithmic averaged *I*−*V* curves of apo-Az at temperatures from 268 to 368 K. (d) Currents of apo-Az at +0.5 V as a function of inverse temperature. The black curves in panels a and c are for the samples after denaturation. They correspond to the circled points in panels b and d, respectively. Error bars were calculated by the standard deviation of *I*−*V* curve measurements for each temperature.

In the CP-AFM measurements, we observed a constant adhesion force of 5 nN, which was measured as the snap-out force during retraction of the AFM tip. Thus, the total load applied on the proteins is 11 nN. In the macroscopic measurement using an Au pad, the force, exerted by the Au on the proteins, is mainly governed by the intrinsic adhesion force. Symmetry considerations imply that this force is similar to that of this intrinsic metal tip/protein adhesion. Since in the macroscopic scale measurements there is no significant additional external load, the effective pressure applied to each protein molecule is less than half that in the nanoscale measurements.

The role of the Cu redox center in the ETp process across the protein was measured on a monolayer of apo-Az. Similar (optical) heights were deduced from ellipsometry for apo-Az and holo-Az (18 Å), comparable to the observed height on the Si surfaces[20] corresponding to similar packing of the monolayer on the Au surface. The junctions of apo-Az were prepared similarly to those of holo-Az, and the same AFM tips were used to measure the *I*−*V* characteristics of the two proteins. Figure 4c shows the *I*−*V* curves of the apo-Az junction on a logarithmic current scale at different temperatures, in the range of 248−368 K. Figure 4d shows the logarithm of the currents through the junctions at +0.5 V as a function of inverse temperature. A linear dependence is clearly observed. Thus, removing the Cu ion changes the dominant mechanism of ETp across the protein from temperature-independent to the more common thermally activated type, in agreement with the macroscopic ETp results.[21]

Upon raising the temperature further we observed a sharp irreversible decrease of the currents for apo- and holo-Az junctions (marked in the circle in Figure 4b,d). This is in contrary to the reversible temperature dependence that we observe (by heating and cooling) in the monolayer junction at lower temperatures. The most likely reason for the irreversible decrease in the currents is the denaturation of the protein. The reported T_m values of apo- and holo-Az in solution are 335 and 355 K, respectively,[43] which are slightly lower than the those of the observed denaturation in the macro- and nanoscale measurement. Higher stability, consequently leading to higher T_m, has also been observed previously in other dry proteins.[44] In our macroscopic scale experiments these current drops appear at 350 and 360 K for apo and holo-Az, respectively.[21] The differences in denaturation temperatures by 5−15 K may be due to the immobilization of the proteins *via* disulfide bonds, which may increase the stability of the protein.[45]

The effect of applied tip force on the current as a function of temperature is shown in Figure 5 panels a and b, which give the currents at +0.5 V applied bias on the tip as a function of inverse temperatures for holo- and apo-Az, respectively, at 6, 9, and 12 nN tip force. As shown in Figure 3 for room temperature currents, increasing the force leads to higher current. However,

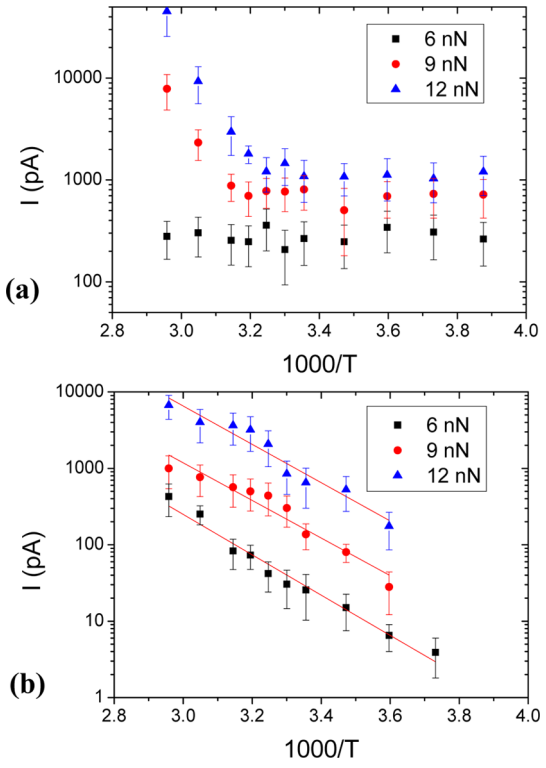

Figure 5. ETp temperature dependence for (a) holo-Az and (b) apo-Az junctions, shown as plots of current at 0.5 V (logarithmic scale) *vs* inverse temperature at 6, 9, and 12 nN applied tip force. Error bars are based on the standard deviation of the "Peak Force" currents from current mapping.

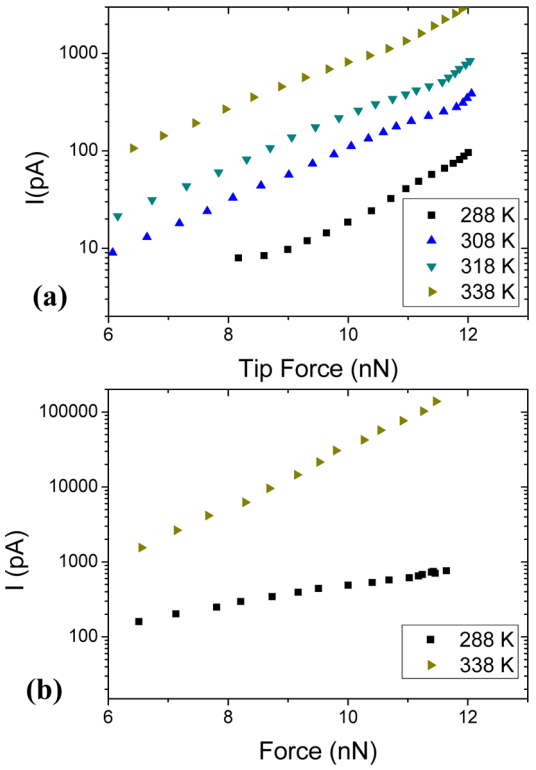

Figure 6. Representative single measurement, current–force curves (logarithmic scale) at 0.5 V at different temperatures for (a) apo-Az and (b) holo-Az junctions. The slopes of the logarithmic current *vs* force plots are 0.6 ± 0.1 for apo-Az for all temperatures and 0.4 ± 0.1 at 288 K and 0.9 ± 0.2 at 338 K for holo-Az. The currents at 288 K at the lowest forces reflect the sensitivity limit for single measurements (10 pA).

we find a distinct difference in the temperature dependence of the current between apo- and holo-Az, at different tip forces. While currents *via* apo-Az increase with increasing tip force, as expected from a decrease in the tip–substrate distance, their temperature dependence remains similar. By fitting the curves in Figure 5b to the Arrhenius equation, we can estimate the ETp activation energy, E_a, of apo-Az to be 600 ± 100 meV at all of the applied forces. In contrast, the currents *via* holo-Az change from temperature-**in**dependent at 6 nN to thermally activated at higher applied forces (9 and 12 nN) at temperatures greater than 310 K. Below 310 K the currents through holo-Az remain temperature-independent at all of the applied forces, but currents are higher for higher applied force, which can be the result of a decrease in tip–substrate distance. These differences between apo- and holo-Az can also be seen in a plot of the measured currents as a function of the applied tip force (Figure 6), obtained by combining simultaneous force and current traces as a function of time by high speed data acquisition in Peak Force TUNA mode. Our results show that while the slopes of the currents as a function of the tip force for apo-Az (Figure 6a) remain similar at different temperatures, the slope for holo-Az increased significantly with temperature.

The above-mentioned irreversible drop in current upon heating was observed at similar temperatures for both holo-Az and apo-Az, with 6, 9, and 12 nN tip force applied. This similarity suggests that any structure distortion of the protein caused by a tip force of up to 12 nN is minor, compared to the change involved in denaturation.

DISCUSSION

Comparison of Current Densities Observed in Azurin and Molecular Wires. Thermally activated ETp was previously observed in CP-AFM studies *via* >4 nm long conjugated molecules (with temperature-independent behavior for shorter molecules).[46,47] The Arrhenius plots of the currents as a function of inverse temperature observed in those experiments were interpreted in terms of a hopping ETp mechanism. This may well be the dominant ETp mechanism *via* apo-Az. While Az, with or without its Cu redox center, is not a conjugated system, apo-Az behaves *qualitatively* in a similar fashion to conjugated molecules ("molecular wires"), but with measured currents of tens of pA, rather than the μA currents that flow through conjugated molecules of similar molecular length at 0.5 V applied bias.[47] The contact area for these conjugated molecules was estimated at 50 nm^2.[47] We can estimate our contact area by using the following relation derived from

Herzian contact mechanics:[24]

$$A = \pi\left(\frac{3P_{\text{eff}}}{4E^*}r\right)^{2/3}$$

where r is the tip radius, P_{eff} is the load, and E^* is the effective modulus, which we estimate to be ~100 MPa.[48,49] From this calculation we assess the contact area in our studies to be ~450 nm^2. After normalization of the contact area differences, we find the current densities for both holo- and apo-Az to be 5−6 orders of magnitude lower than those of conjugated molecules. In comparison, an insulating layer of alkyl chains of similar thickness, at comparable force and tip radius should pass 10^{-18} A (extrapolating from CP-AFM measurement on $CH_3(CH_2)_{11}SH$, ~500 pA at 0.5 V, and using β = 1.1 A^{-1}[25]). This observation by itself makes proteins, in terms of conductivity, more akin to molecular wires than to insulators.

Current Densities at Macro- *versus* Nanoscale Contacts. In general, the CP-AFM current−temperature behavior of Az with nanoscale electrode contact is consistent with our previously reported macroscopic results,[21] in having them exhibit a temperature-independent ETp *via* holo-Az and thermally activated ETp *via* apo-Az. There are however some differences between the CP-AFM and the macroscopic conductance measurements[25] in the normalized current densities across the proteins (see below) and in the value of the activation energy, E_a, of apo-Az.

From the nanoscale measurements (AFM tip radius of 20 nm) we calculate for holo-Az junctions a current density of ~100 A/cm^2 at 1 V, while in the macroscopic measurements (contact area of 0.2 mm^2) it was ~3 × 10^{-3} A/cm^2, namely five orders of magnitude lower. We ascribe this difference to differences in the way the proteins are immobilized between the two electrodes in the two measurements. In the macroscopic conductance measurements the substrate was a p^{+2}-Si surface with a 1 nm thick layer of silicon oxide, with, as linker, a self-assembled monolayer of a C_3 organo-silane on top of it. The linker molecules were covalently bound to the Az proteins *via* a disulfide bond.[20] The top electrode was a macroscopic pad of gold (~0.2 mm^2), deposited by the lift-off, float-on (LOFO) technique,[50] to contact the protein layer. Thus, in the macroscopic measurements the two contacts were separated not only by the protein monolayer, but also by two additional insulating layers, silicon oxide, and organic linker, with a combined thickness of ~16 Å). These two additional insulating layers will decrease the currents by some 5 orders of magnitude, assuming a current decay factor (for insulating molecular layers) of β = 0.7 A^{-1}.[12]

Thermal Activation Energy for ETp *via* apo-Az. The distinct experimental setups may also be the cause for the different calculated ETp activation energies of apo-Az, that is, 320 meV from the macroscopic measurements[30] and ~600 meV from the CP-AFM measurements. Because the holo-Az results exhibited the same temperature-independent behavior in the two different experimental setups, it is very unlikely that the different electrodes are the cause for this difference in activation energy. A possible reason is that the covalent S−S bond between one of the two exposed cysteines and SH group of the linker in the macroscopic measurements is stronger than the Au−S bond that binds the protein to the Au substrate in the CP-AFM measurements. The smaller coupling to the electrode might allow additional vibration modes at the Au/protein interface, which are hindered in the case of the disulfide bridge bond that holds the protein in the macroscopic configuration.

Tip Pressure Dependence of the ETp. A striking result of this study is the observed distinct temperature dependence of the current through holo-Az as a function of applied force (Figures 5 and 6). As discussed previously, the higher sensitivity to the applied tip force of currents through apo-Az (at room temperature) than through holo-Az, (Figure 3) is interpreted as being a result of the increased flexibility of apo-Az, compared to holo-Az. This increased flexibility of apo-Az causes the tip−surface separation distance to be smaller at high forces than in the holo-Az surface, which explains the larger increase in currents with increasing force *via* apo-Az. In other words, Young's modulus of apo-Az protein is lower than holo-Az, leading to a more significant change in the separation distance between the tip and the gold substrate, due to protein compression, hence leading to more pronounced changes in currents between the electrodes.

An increase in the applied tip force on top of the holo-Az monolayer results in the AFM tip pushing toward the Cu binding site (which is located on the tip-side of the junction as shown in the scheme of Figure 1). Marshall *et al.*[51] have shown that minor alterations of the hydrogen-bonding network in the second coordination sphere of the Cu site may cause pronounced changes in the ET properties of holo-Az, which consequently can change its flexibility.[52−54] The change (at T > 310 K) from temperature-independent to thermally activated ETp *via* holo-Az suggests a relation between the protein structure and flexibility, and the mechanism of ETp through it.[55] The suggested correlation between flexibility and conductivity[51] has been indicated by measurements of ETp *via* peptide nucleic acid monolayers, where attenuation in currents was observed for structures comprising the same sequence, with and without methylation, a modification that increases the structural rigidity.[56] Therefore, we suggest that the protein's flexibility (in the case of holo-Az), together with the temperature of the system (for apo-Az) are dominant parameters that control both the mechanism and the efficiency of ETp *via* the protein. This is demonstrated in the pivotal change of

ETp *via* holo-azurin. We postulate that if a force of 9 nN or higher is applied to the tip, the perturbation in the secondary structure that results from the increase in tip force from 6 to 9 nN causes major changes in the temperature dependence of the (high temperature) currents. As a result the ETp mechanism becomes more similar to that for Apo-azurin. The recent work by Zaballa *et al*. supports our postulate regarding ETp, by showing that the presence of the Cu ion greatly increases the rigidity of the binding site of Az, which consequently minimizes the reorganization energy and enhances ETp (and ET) efficiency.[40]

The impact of applied forces on the ETp characteristics of proteins suggests that the compressive and tensile stress applied to the examined protein need to be taken into consideration when its electrical conduction properties are investigated. In similar ETp measurements that were conducted *via* alkyl chains, currents began to increase only at >12 nN tip force,[25] suggesting a more rigid structure than that of proteins. Furthermore, the force applied by the tip on an alkyl chain has apparently a simpler effect than that on proteins, where more complex secondary structures can be affected. *Thus, consideration of the applied force appears to be particularly relevant for nanoscopic approaches, such as STM and CP-AFM, for measurements of proteins, as shown here*.

CONCLUSIONS

CP-AFM measurements of protein monolayers show that, at low tip-force, ETp through holo-Az is temperature-independent over a significant range of temperatures (248−373 K), while for apo-Az the process is thermally activated. This observed difference is in line with our earlier macroscopic ETp results and with long-range temperature-independent intramolecular electron transfer in holo-azurin in this range of temperatures.[57] As the tip-force increases, ETp through holo-Az changes from temperature-independent to thermally activated at higher temperatures (>310 K). It is likely that the mechanism of ETp through apo-Az does not change with pressure, as the thermal activation energy does not change. The currents, though, increase with increasing tip force, an effect that can by ascribed to decreases of through-space ETp gaps (by compression of tunneling pathways) in the protein, consistent with results of Meier *et al*.[58] The results obtained with holo-Az do suggest a pressure-induced change in ETp mechanism at temperatures >310 K, which may be due to a pressure-induced change in protein structure. This assumption correlates with ETp results across plastocyanin with force-dependent CP-AFM,[26] which showed that structural changes occur if >8 nN force is applied to the tip, a force similar to that around which we find the change in ETp mechanism for holo-Az.

Even though this change is likely to be minor, because it does not significantly alter the denaturation temperature, it does manifest itself in ETp. Thus, this result illustrates the remarkable sensitivity of ETp to both relatively minor structural changes, as well as to major changes in the protein (denaturation). The strong relation between protein flexibility and applied force, and its impact on the temperature-dependence of ETp *via* Az, indicates the importance of the applied forces for current measurements in scanning microscopy configurations (*cf.*, review on biomolecule conductance[11] and report on force-dependent conductivity[14]).

Finally, our observation directly points to a general issue that is worth considering: force-mediated effects in nanoscale electrical measurements. The applied forces should be the lowest that still ensure reproducible ETp. Because a change in applied force such as the one demonstrated here can affect ETp, changes in force during ETp measurements should be avoided or their effect should be considered.

This consideration is especially important for ETp measurements through proteins because of the relative ease by which they can change conformation compared to more rigid molecules, such as, for example, conjugated or alkyl ones. The combination of controlled temperature and environment and a defined (and reported) tip diameter and force are critical parameters that define the initial conditions of the system, and, hence, the output of the measurement.

METHODS

Preparation of the Substrates. Silicon wafers (p type, boron doped, ⟨100⟩ single side polished, $\rho < 0.001\ \Omega\cdot$cm), were sonicated for 2 min with ethyl acetate, acetone, and ethanol. Immediately after that, the wafer was etched for 1 min with 2% HF, washed with Milli-Q (18 MΩ) water and cleaned again with fresh piranha solution for 20 min (7/3 v/v of H_2SO_4/H_2O_2) at 80°. After being cleaned with piranha, the wafers were rinsed thoroughly with Milli-Q and etched with 2% HF again, resulting in a Si−H surface termination. The wafers were immediately stored in a container filled with nitrogen. The samples were loaded into an e-beam evaporator and, when a vacuum of $<5 \times 10^{-6}$ mbar was reached, 2 nm of Cr (serving as an adhesion layer) followed by 50 nm of Au were evaporated with a deposition rate of 1 Å/s. The gold-coated Si samples were then cut into 1×1 cm^2 slides, and cleaned for 10 min with UV/ozone treatment followed by a 30 min immersion in ethanol.[59]

Preparation and Characterization of the Proteins. Azurin was isolated from *Alcaligenes faecalis* by the method of Ambler and Wynn.[60] Apo-Az solution was prepared as described.[20] Holo-Az and apo-Az monolayers were prepared by immersing the gold substrates in a ∼1 mg/mL solution of azurin in 50 mM ammonium acetate (NH_4Ac) buffer (pH 4.6) for 2 h followed by rinsing in clean H_2O and drying under a fine nitrogen stream. The protein monolayers were characterized by ellipsometry that yielded 1.8 nm optical thickness, which corresponds to values

obtained in our previous studies of Az on Si surfaces.[20] The actual thickness is 3.5 nm, as found by AFM (Supporting Information, Figure S1b)

AFM Imaging. The topography of the self-assembled monolayer of proteins was characterized by AFM in semicontact mode under a N_2 purge. A Solver P47 SPM system (ND-MDT, Zelenograd Russia) and Pt-coated Si probes (NSC36, 75kHz, 0.6 N/m, MIKROMASCH) were used. The topography images and the phase images were taken simultaneously at a scan rate of 1 Hz. The applied force from the tip on the proteins, during the topography imaging, is at least 1 order of magnitude smaller than those used for CP-AFM measurements (Supporting Information).

CP-AFM Measurements as a Function of Temperature. The CP-AFM measurements as a function of temperature were performed with a Multimode/Nanoscope V system (Bruker-Nano, Santa Barbara, CA USA) under constant N_2 flow purge. All-metal Pt AFM probes with nominal force constant of 0.8 N/m (25PT300B, Rocky Mountain Nanotechnology, Salt Lake City, Utah USA) and tip radius of 20 nm, were used for the CP-AFM measurements. The probes were brought into contact with the self-assembled protein monolayer using a constant force feedback (contact mode). A tip force of 6 nN was used to avoid changes in the protein, following ref 19. Temperature was controlled by a Bruker heater/cooling system that uses an inert atmosphere flow, rather than a closed vacuum system as in the case of our macroscopic measurements. With this setup we can obtain current voltage ($I-V$) curves between 248 and 373 K. At temperatures below 273 K (0 °C) the protein surface was monitored constantly to verify that no ice is formed, ascertaining the low moisture level in the system. For each temperature, the $I-V$ measurements were performed only after the system had stabilized and remained stable for at least 30 min. Thirty $I-V$ curves over an area of $1 \times 1\ \mu m^2$ were taken and averaged for each temperature. The drifting of the tip position does not affect our measurements. Whenever drastic current drops occurred, the tip was cleaned, using a high voltage pulse (-10 to $+10$ V in 0.1 s). The tip force was constant during the measurements.

AFM Peak Force TUNA Mode. An extension module for current measurement was used to enable the current mapping under AFM Peak Force (PF-TUNA) mode. In Peak Force TUNA mode, the probe was cycled in and out of contact with the surface at 1 or 2 kHz, while the tip is scanned across the sample at a rate of 1 Hz per scan line. The fast data acquisition, coupled with feedback loop control, gave the maximum force on the tip for each individual cycle. Current, force, and other mechanical properties are recorded during these controlled tip–sample contact cycles. Peak current is recorded at maximum force applied to the sample (Peak Force set point). Measurements were performed in both imaging mode and spectroscopy mode. In the imaging mode, a current map is acquired simultaneously with topography at a tip bias of +0.5 V with a tip Peak Force of 6, 9, and 12 nN. The currents from the image were averaged for each such mapping at a given temperature. In spectroscopy mode, the tip was ramped into and out of the surface at high cycling frequency (1 kHz), while recording simultaneously both force and current as a function of time. The current force curve was plotted by combining the two simultaneous traces.

Conflict of Interest: The authors declare no competing financial interest.

Acknowledgment. W.L. thanks Daniel Frisbie and Liang Luo (Univ. Minnesota) for helpful guidance with, and discussions on, CP-AFM measurement procedures. L.S. thanks the Eshkol program for financial support. N.A. thanks the Clore program for financial support. We thank the Minerva Foundation (Munich), the Kimmelman center for Biomolecular Structure and Assembly, the Kimmel centre for Nanoscale Science, and the Grand Centre for Sensors and Security for partial support. M.S. holds the Katzir-Makineni Chair in Chemistry. D.C. holds the Schaefer Chair in Energy Research.

Supporting Information Available: Additional information about AFM imaging, AFM tip scratching procedure, protein thickness measurements, and raw data of $I-V$ curves for Az and apo-Az at room temperature. This material is available free of charge *via* the Internet at http://pubs.acs.org.

REFERENCES AND NOTES

1. Farver, O.; Pecht, I., Elucidation of Electron-Transfer Pathways in Copper and Iron Proteins by Pulse Radiolysis Experiments. In *Progress in Organic Chemistry;* Karlin, K. D., Ed.; 2007; Vol. *55*, pp 1–78.
2. Gray, H. B.; Winkler, J. R. Electron Tunneling through Proteins. *Q. Rev. Biophys.* **2003**, *36*, 341–372.
3. Regan, J. J.; Dibilio, A. J.; Langen, R.; Skov, L. K.; Winkler, J. R.; Gray, H. B.; Onuchic, J. N. Electron-Tunneling in Azurin—The Coupling across a Beta-Sheet. *Chem. Biol.* **1995**, *2*, 489–496.
4. Chi, Q. J.; Zhang, J. D.; Andersen, J. E. T.; Ulstrup, J. Ordered Assembly and Controlled Electron Transfer of the Blue Copper Protein Azurin at Gold (111) Single-Crystal Substrates. *J. Phys. Chem. B* **2001**, *105*, 4669–4679.
5. Chi, Q. J.; Zhang, J. D.; Nielsen, J. U.; Friis, E. P.; Chorkendorff, I.; Canters, G. W.; Andersen, J. E. T.; Ulstrup, J. Molecular Monolayers and Interfacial Electron Transfer of *Pseudomonas aeruginosa* Azurin on Au(111). *J. Am. Chem. Soc.* **2000**, *122*, 4047–4055.
6. Gaigalas, A. K.; Niaura, G. Measurement of Electron Transfer Rates between Adsorbed Azurin and a Gold Electrode Modified with a Hexanethiol Layer. *J. Colloid Interface Sci.* **1997**, *193*, 60–70.
7. Jeuken, L. J. C.; Armstrong, F. A. Electrochemical Origin of Hysteresis in the Electron-Transfer Reactions of Adsorbed Proteins: Contrasting Behavior of the "Blue" Copper Protein, Azurin, Adsorbed on Pyrolytic Graphite and Modified Gold Electrodes. *J. Phys. Chem. B* **2001**, *105*, 5271–5282.
8. Alessandrini, A.; Corni, S.; Facci, P. Unravelling Single Metalloprotein Electron Transfer by Scanning Probe Techniques. *Phys. Chem. Chem. Phys.* **2006**, *8*, 4383–4397.
9. Friis, E. P.; Andersen, J. E. T.; Madsen, L. L.; Moller, P.; Ulstrup, J. *In Situ* STM and AFM of the Copper Protein *Pseudomonas aeruginosa* Azurin. *J. Electroanal. Chem.* **1997**, *431*, 35–38.
10. Andolfi, L.; Bruce, D.; Cannistraro, S.; Canters, G. W.; Davis, J. J.; Hill, H. A. O.; Crozier, J.; Verbeet, M. P.; Wrathmell, C. L.; Astier, Y. The Electrochemical Characteristics of Blue Copper Protein Monolayers on Gold. *J. Electroanal. Chem.* **2004**, *565*, 21–28.
11. Shinwari, M. W.; Deen, M. J.; Starikov, E. B.; Cuniberti, G. Electrical Conductance in Biological Molecules. *Adv. Funct. Mater.* **2010**, *20*, 1865–1883.
12. Ron, I.; Pecht, I.; Sheves, M.; Cahen, D. Proteins as Solid-State Electronic Conductors. *Acc. Chem. Res.* **2010**, *43*, 945–953.
13. Das, R.; Kiley, P. J.; Segal, M.; Norville, J.; Yu, A. A.; Wang, L. Y.; Trammell, S. A.; Reddick, L. E.; Kumar, R.; Stellacci, F.; *et al.* Integration of Photosynthetic Protein Molecular Complexes in Solid-State Electronic Devices. *Nano Lett.* **2004**, *4*, 1079–1083.
14. Zhao, J. W.; Davis, J. J. Force Dependent Metalloprotein Conductance by Conducting Atomic Force Microscopy. *Nanotechnology* **2003**, *14*, 1023–1028.
15. Davis, J. J.; Peters, B.; Xi, W. Force Modulation and Electrochemical Gating of Conductance in a Cytochrome. *J. Phys. Condens. Matter* **2008**, 20.
16. Davis, J. J.; Wang, N.; Morgan, A.; Zhang, T. T.; Zhao, J. W. Metalloprotein Tunnel Junctions: Compressional Modulation of Barrier Height and Transport Mechanism. *Faraday Discuss.* **2006**, *131*, 167–179.
17. Davis, J. J.; Wrathmell, C. L.; Zhao, J.; Fletcher, J. The Tunnelling Conductance of Molecularly Ordered Metalloprotein Arrays. *J. Mol. Recognit.* **2004**, *17*, 167–173.
18. Zhao, J. W.; Davis, J. J. Molecular Electron Transfer of Protein Junctions Characterised by Conducting Atomic Force Microscopy. *Colloids Surf., B* **2005**, *40*, 189–194.
19. Zhao, J. W.; Davis, J. J.; Sansom, M. S. P.; Hung, A. Exploring the Electronic and Mechanical Properties of Protein Using Conducting Atomic Force Microscopy. *J. Am. Chem. Soc.* **2004**, *126*, 5601–5609.
20. Ron, I.; Sepunaru, L.; Itzhakov, S.; Belenkova, T.; Friedman, N.; Pecht, I.; Sheves, M.; Cahen, D. Proteins as Electronic Materials: Electron Transport through Solid-State Protein Monolayer Junctions. *J. Am. Chem. Soc.* **2010**, *132*, 4131–4140.

21. Sepunaru, L.; Pecht, I.; Sheves, M.; Cahen, D. Solid-State Electron Transport across Azurin: From a Temperature-Independent to a Temperature-Activated Mechanism. *J. Am. Chem. Soc.* **2011**, *133*, 2421–2423.
22. Bizzarri, A. R.; Andolfi, L.; Taranta, M.; Cannistraro, S. Optical and Electronic Coupling of the Redox Copper Azurin on ITO-Coated Quartz Substrate. *Biosens. Bioelectron.* **2008**, *24*, 204–209.
23. Mentovich, E. D.; Belgorodsky, B.; Richter, S. Resolving the Mystery of the Elusive Peak: Negative Differential Resistance in Redox Proteins. *J. Phys. Chem. Lett.* **2011**, *2*, 1125–1128.
24. Engelkes, V. B.; Beebe, J. M.; Frisbie, C. D. Analysis of the Causes of Variance in Resistance Measurements on Metal−Molecule−Metal Junctions Formed by Conducting-Probe Atomic Force Microscopy. *J. Phys. Chem. B* **2005**, *109*, 16801–16810.
25. Wold, D. J.; Frisbie, C. D. Fabrication and Characterization of Metal−Molecule−Metal Junctions by Conducting Probe Atomic Force Microscopy. *J. Am. Chem. Soc.* **2001**, *123*, 5549–5556.
26. Andolfi, L.; Cannistraro, S. Conductive Atomic Force Microscopy Study of Plastocyanin Molecules Adsorbed on Gold Electrode. *Surf. Sci.* **2005**, *598*, 68–77.
27. Good, R. H. J.; Muller, E. W. *Handbuch Der Physik;* Springer Verlag: Berlin, 1956; Vol. XXI.
28. Xu, D.; Watt, G. D.; Harb, J. N.; Davis, R. C. Electrical Conductivity of Ferritin Proteins by Conductive AFM. *Nano Lett.* **2005**, *5*, 571–577.
29. Stamouli, A.; Frenken, J. W. M.; Oosterkamp, T. H.; Cogdell, R. J.; Aartsma, T. J. The Electron Conduction of Photosynthetic Protein Complexes Embedded in a Membrane. *FEBS Lett.* **2004**, *560*, 109–114.
30. Rakshit, T.; Mukhopadhyay, R. Solid-State Electron Transport in Mn-, Co-, Holo-, and Cu-Ferritins: Force-Induced Modulation Is Inversely Linked to the Protein Conductivity. *J. Colloid Interface Sci.* **2012**, *388*, 282–292.
31. Marcus, R. A.; Sutin, N. Electron Transfers in Chemistry and Biology. *Biochim. Biophys. Acta* **1985**, *811*, 265–322.
32. In our macroscopic measurements the force, applied by the contact pad, which is primarily due to adhesion forces, translates into a fixed force applied to the protein.
33. Tao, N. J. Probing Potential-Tuned Resonant Tunneling through Redox Molecules with Scanning Tunneling Microscopy. *Phys. Rev. Lett.* **1996**, *76*, 4066–4069.
34. Bar, G.; Thomann, Y.; Brandsch, R.; Cantow, H. J.; Whangbo, M. H. Factors Affecting the Height and Phase Images in Tapping Mode Atomic Force Microscopy. Study of Phase-Separated Polymer Blends of Poly(ethene-*co*-styrene) and Poly(2,6-dimethyl-1,4-phenylene oxide). *Langmuir* **1997**, *13*, 3807–3812.
35. Kuhle, A.; Sorensen, A. H.; Bohr, J. Role of Attractive Forces in Tapping Tip Force Microscopy. *J. Appl. Phys.* **1997**, *81*, 6562–6569.
36. San Paulo, A.; Garcia, R. Amplitude, Deformation and Phase Shift in Amplitude Modulation Atomic Force Microscopy: A Numerical Study for Compliant Materials. *Surf. Sci.* **2001**, *471*, 71–79.
37. Shepard, W. E. B.; Kingston, R. L.; Anderson, B. F.; Baker, E. N. Structure of Apo-Azurin from *Alcaligenes-denitrificans* at 1.8-Angstrom Resolution. *Acta Crystallogr., Sect. D: Biol. Crystallogr.* **1993**, *49*, 331–343.
38. Nar, H.; Messerschmidt, A.; Huber, R.; Vandekamp, M.; Canters, G. W. Crystal-Structure of *Pseudomonas-aeruginosa* Apo-Azurin at 1.85 Angstrom Resolution. *FEBS Lett.* **1992**, *306*, 119–124.
39. Vandekamp, M.; Canters, G. W.; Wijmenga, S. S.; Lommen, A.; Hilbers, C. W.; Nar, H.; Messerschmidt, A.; Huber, R. Complete Sequential H-1 and N-15 Nuclear-Magnetic-Resonance Assignments and Solution Secondary Structure of the Blue Copper Protein Azurin from *Pseudomonas-aeruginosa*. *Biochemistry* **1992**, *31*, 10194–10207.
40. Zaballa, M.-E.; Abriata, L. A.; Donaire, A.; Vila, A. J. Flexibility of the Metal-Binding Region in Apo-Cupredoxins. *Proc. Natl. Acad. Sci. U.S.A.* **2012**, *109*, 9254–9259.
41. Rakshit, T.; Banerjee, S.; Mukhopadhyay, R. Near-Metallic Behavior of Warm Holoferritin Molecules on a Gold(111) Surface. *Langmuir* **2010**, *26*, 16005–16012.
42. Maruccio, G.; Marzo, P.; Krahne, R.; Passaseo, A.; Cingolani, R.; Rinaldi, R. Protein Conduction and Negative Differential Resistance in Large-Scale Nanojunction Arrays. *Small* **2007**, *3*, 1184–1188.
43. Engeseth, H. R.; McMillin, D. R. Studies of Thermally Induced Denaturation of Azurin and Azurin Derivatives by Differential Scanning Calorimetry: Evidence for Copper Selectivity. *Biochemistry* **1986**, *25*, 2448–2455.
44. Shen, Y.; Safinya, C. R.; Liang, K. S.; Ruppert, A. F.; Rothschild, K. J. Stabilization of the Membrane Protein Bacteriorhodopsin to 140 °C in Two-Dimensional Films. *Nature* **1993**, *366*, 48–50.
45. Bonander, N.; Leckner, J.; Guo, H.; Karlsson, B. G.; Sjölin, L. Crystal Structure of the Disulfide Bond-Deficient Azurin Mutant C3a/C26a. *Eur. J. Biochem.* **2000**, *267*, 4511–4519.
46. Luo, L.; Choi, S. H.; Frisbie, C. D. Probing Hopping Conduction in Conjugated Molecular Wires Connected to Metal Electrodes. *Chem. Mater.* **2010**, *23*, 631–645.
47. Choi, S. H.; Frisbie, C. D. Enhanced Hopping Conductivity in Low Band Gap Donor-Acceptor Molecular Wires up to 20 Nm in Length. *J. Am. Chem. Soc.* **2010**, *132*, 16191–16201.
48. Atsushi, I. Local Rigidity of a Protein Molecule. *Biophys. Chem.* **2005**, *116*, 187–191.
49. Wolfram|Alpha. Http://Www.Wolframalpha.Com/Input/?I=Biological+Material&Lk=1&a=Clashprefs_*Materialclass.Biologicalmaterial- (accessed July 17, 2012).
50. Vilan, A.; Cahen, D. Soft Contact Deposition onto Molecularly Modified GaAs. Thin Metal Film Flotation: Principles and Electrical Effects. *Adv. Funct. Mater.* **2002**, *12*, 795–807.
51. Marshall, N. M.; Garner, D. K.; Wilson, T. D.; Gao, Y. G.; Robinson, H.; Nilges, M. J.; Lu, Y. Rationally Tuning the Reduction Potential of a Single Cupredoxin Beyond the Natural Range. *Nature* **2009**, *462*, 113–116.
52. Benning, M. M.; Meyer, T. E.; Rayment, I.; Holden, H. M. Molecular Structure of the Oxidized High-Potential Iron−Sulfur Protein Isolated from *Ectothiorhodospira vacuolata*. *Biochemistry* **1994**, *33*, 2476–2483.
53. Palfey, B. A.; Basu, R.; Frederick, K. K.; Entsch, B.; Ballou, D. P. Role of Protein Flexibility in the Catalytic Cycle of *p*-Hydroxybenzoate Hydroxylase Elucidated by the Pro293ser Mutant. *Biochemistry* **2002**, *41*, 8438–8446.
54. Battistuzzi, G.; Borsari, M.; Cowan, J. A.; Ranieri, A.; Sola, M. Control of Cytochrome C Redox Potential: Axial Ligation and Protein Environment Effects. *J. Am. Chem. Soc.* **2002**, *124*, 5315–5324.
55. Beratan, D. N.; Skourtis, S. S.; Balabin, I. A.; Balaeff, A.; Keinan, S.; Venkatramani, R.; Xiao, D. Q. Steering Electrons on Moving Pathways. *Acc. Chem. Res.* **2009**, *42*, 1669–1678.
56. Wierzbinski, E.; de Leon, A.; Davis, K. L.; Bezer, S.; Wolak, M. A.; Kofke, M. J.; Schlaf, R.; Achim, C.; Waldeck, D. H. Charge Transfer through Modified Peptide Nucleic Acids. *Langmuir* **2012**, *28*, 1971–1981.
57. Skov, L. K.; Pascher, T.; Winkler, J. R.; Gray, H. B. Rates of Intramolecular Electron Transfer in Ru(Bpy)2(Im)(His83)-Modified Azurin Increase Below 220 K. *J. Am. Chem. Soc.* **1998**, *120*, 1102–1103.
58. Meier, M.; van Eldik, R.; Chang, I. J.; Mines, G. A.; Wuttke, D. S.; Winkler, J. R.; Gray, H. B. Pressure Effects on the Rates of Intramolecular Electron Transfer in Ruthenium-Modified Cytochrome C. Role of the Intervening Medium in Tuning Distant Fe^{2+}:Ru^{3+} Electronic Couplings. *J. Am. Chem. Soc.* **1994**, *116*, 1577–1578.
59. Ron, H.; Matlis, S.; Rubinstein, I. Self-Assembled Monolayers on Oxidized Metals. 2. Gold Surface Oxidative Pretreatment, Monolayer Properties, and Depression Formation. *Langmuir* **1998**, *14*, 1116–1121.
60. Ambler, R. P.; Wynn, M. Amino-Acid Sequences of Cytochromes C-551 from 3 Species of *Pseudomonas*. *Biochem. J.* **1973**, *131*, 485–498.